

Separation of formic acid and acetic acid from aqueous solutions using sugar beet processing fly ash: characterization, kinetics, isotherms and thermodynamics

Hani Zeidan^{a,b}, Damla Ozdemir^b, Nezahat Kose^b, Erol Pehlivan^{a,b}, Gülnare Ahmetli^{a,b}, Mustafa Esen Marti^{a,b,*}

^aDepartment of Chemical Engineering, Konya Technical University, Konya, Turkey, Tel. +90-332-223-1837; Fax: +90-332-241-0635; emails: memarti@ktun.edu.tr/mustafaesenmarti@gmail.com (M.E. Marti), hani-z82@hotmail.com (H. Zeidan), epehlivan@ktun.edu.tr (E. Pehlivan), gahmetli@ktun.edu.tr (G. Ahmetli)

^bDepartment of Chemical Engineering, Selçuk University, Konya, Turkey, emails: dml.ozdmer.hls@gmail.com (D. Ozdemir), nezahat.kose@hotmail.com (N. Kose)

Received 9 December 2019; Accepted 14 May 2020

ABSTRACT

The present study is on the use of sugar beet processing fly ash (SPFA) during the separation of acetic acid (AA) and formic acid (FA) from aqueous solutions by adsorption technique. Kinetic studies showed that the equilibration time was about 70 min for AA while 60 min for FA. The related data were observed to follow the pseudo-second-order kinetic model. Isotherm curves exhibited that the process was fitted with Type 1. The adsorption efficiency increased with the increase in SPFA dosage and decreased with the AA or FA concentration. Equilibrium data were in consistency with the Langmuir isotherm model for both solutes. The adsorption capacities and removal efficiencies obtained with FA were higher than those with AA. The maximum values were 7.00 and 5.60 mmol/g for FA and AA, respectively. These values were considerably higher than the ones previously reported for the adsorption of these acids using several types of synthetic resins and fly ashes. Temperature negatively influenced the process but the effect was not significant. Regardless of the acid type studied, the process was exothermic and spontaneous. The results showed that SPFA can be efficiently used in the separation of these carboxylic acids from aqueous solutions.

Keywords: Sugar beet processing fly ash; Acetic acid; Formic acid; Adsorption; Equilibrium; Kinetics; Thermodynamics

1. Introduction

Aqueous waste streams consisting of organic pollutants must be treated prior to their discharge to the rivers or re-utilization. Carboxylic acids are organic chemicals and frequently encountered in wastewater streams since they are widely used in various industries such as food, pharmaceutical, agriculture, etc [1–3]. Depending on the raw materials, process type and variables, the composition and amount of carboxylic acids in wastewaters change. They are reactive

chemicals and can form toxic chemicals with other materials in the wastewaters. However, their removal combined with their recovery will allow their re-use in industry. As a result, carboxylic acids should be separated from wastewater streams [4–6].

Acetic acid (CH_3COOH , AA) and formic acid (HCOOH , FA) are the simplest carboxylic acids and important raw materials employed in many industries. Acetic acid is mainly used in the production of vinyl acetate and acetic

* Corresponding author.

anhydride. The former is the precursor to the latex emulsion resins, which have many applications in textiles, adhesives, paints, and coatings. Acetic anhydride is primarily utilized in the fabrication of cellulose acetate, which is one of the most important materials in the textile, chemical, health, plastic, and tobacco industries [7–9]. Formic acid is principally employed in textile, dye, leather, rubber, and pharmaceutical industries. Recently, its use in the ensilage of the forage has augmented [8,10]. Because of their widespread applications in various types of industries, effective recovery of AA and FA from aqueous-based media by low-cost means has reached great importance [11–15]. Several types of techniques were established and tested for the separation of these acids from aqueous solutions. Precipitation, electrodialysis, crystallization, liquid-liquid extraction, (reactive) distillation, and adsorption are amongst the methods that have been evaluated for the aim [16–18]. Due to the several disadvantages, most of these methods are not to be accepted to be appropriate for industrial applications. However, adsorption has been claimed to be one of the most promising methods because of its low-cost, selectivity, and environmentally-friendly nature. Its simplicity is also another advantage. In the literature, there are many papers on the separation of low molecular weight carboxylic acids from aqueous-based solutions by adsorption technique. In these studies, generally synthetic resins, especially anionic exchangers, were used [12,14,16,19,20]. They are efficient adsorbents; however, their high cost led the investigators to find cheap and efficient alternatives.

Fly ash is an industrial waste that causes environmental problems [21]. Recently, it has been started to be utilized for several purposes in the industry. In general, it is employed as a filling material in the production of cement and composite materials [22–24]. Its effective usage in the adsorption of several solutes from aqueous solutions was shown in the literature [25–28]. However, there are a few studies on the use of fly ash in the adsorptive separation of organic acids from aqueous phases [29–31]. Kannan and Xavier [29] mixed fly ash with activated carbon and used this mixture for the separation of AA from aqueous solutions. Unfortunately, the authors did not mention the source of the fly ash in their publication. It was observed that the adsorption efficiency increased with the decreases in the AA concentration and particle size. On the other hand, it increased with the contact time and adsorbent dose. The researchers mentioned that the kinetic data were well described with the pseudo-first-order (PFO) kinetic model. In another study, Nawle and Patil [30] used the fly ash attained by the removal of the solids from the flue gases in an electrostatic precipitator through the combustion of coal in a boiler, during the separation of AA from aqueous phases. Their data were in consistency with the Freundlich isotherm, which proposes a physical interaction and multi-layer formation on the adsorbent surface. The authors also added that process efficiency increased with the adsorbent dose. Different from the previous study, a similar trend was observed with the acid concentration. Soni et al. [31] employed bagasse fly ash for the removal of glycolic acid from aqueous phases. Most of the trends reached in this detailed study were similar and consistent with those reported by previous researchers. Isotherm

analysis showed that the highest value of the determination coefficient (R^2) was obtained with the Freundlich isotherm model. The kinetics of the process was observed to be well described by Elovich, pseudo-second-order (PSO) and intraparticle diffusion (ID) models. The thermodynamics showed that the process had an exothermic nature.

In this comparative study, fly ash obtained from sugar beet processing was used as the adsorbent during the adsorptive separation of AA and FA from aqueous single acid solutions. The type of the process, in which the fly ash is obtained, is critical for the performance of the waste material. Effects of process parameters such as contact time, initial acid concentration, adsorbent dose and temperature on the adsorption efficiency and capacity were investigated. The experimental data were used to determine the constants of the kinetic- and isotherm models and thermodynamic parameters. The results were compared for the two acids studied and also with the data previously reported in the literature.

2. Materials and methods

2.1. Materials

The sugar beet processing fly ash (SPFA) utilized as the adsorbent in this study was obtained from a local sugar factory in Konya, Turkey. It was used in the experiments without any pre-treatment other than sieving (particle size < 53 mesh). The carboxylic acids, AA (100% purity, CAS 64-19-7) and FA (99.5% purity, CAS 64-18-6) were supplied by Merck Co., USA. Ultra-high pure (UHP) water, obtained by Millipore Direct-Q System (USA) was used in the experiments. Aqueous solutions of the solutes were prepared by using the carboxylic acids and UHP water.

2.2. Characterization and analysis

The Fourier-transform infrared (FTIR) spectra of raw- and acid-loaded SPFA were obtained via a Bruker Vertex 70 FTIR spectrometer (Bruker Co., Germany) using KBr pellets. The spectra were collected in the range of 4,000–400 cm^{-1} . The surface features and the ratio of the elements of SPFA were examined by scanning electron microscopy (SEM) and energy-dispersive X-ray (EDX) spectroscopy instruments (SEM, Zeiss EVO/LS10, Carl Zeiss AG Co., Germany; EDX, Bruker 123 eV Quantax Microanalysis System, Bruker Co., Germany).

2.3. Assay

The concentrations of the AA and FA in the aqueous phase were determined by an Agilent LC 1220 (Agilent Co., USA). The temperature of the column was 30°C and the detection of the carboxylic acids was performed at 210 nm. The “pH 2.8–0.05 mol/L KH_2PO_4 + 1% $\text{C}_2\text{H}_3\text{N}$ ” solution was used as the mobile phase and the flow rate was 1.25 mL/min. All experiments were repeated twice to ensure data integrity and each sample was analyzed twice. The relative uncertainties of the repeated experiments and analyses were less than 1%. Averages were employed in the calculations [8,12,32].

2.4. Kinetics

Kinetic studies were executed to observe the effect of the contact period and determine the equilibrium time. The experiments were carried out by weighing a fixed amount of SPFA (0.2 g) and adding into 100 mL glass flasks containing 10 mL of 0.25 mol/L AA or FA solution. Samples were taken out every 5 min for 3 h, centrifuged and analyzed for the amount of AA or FA left in the aqueous phase. Kinetic data were tried to be described by four different kinetic models, which were Elovich, PFO, PSO, and Weber–Morris ID models.

2.5. Equilibrium

A constant temperature shaker bath was utilized in the adsorption experiments. Aqueous solutions of FA and AA having varied initial concentrations (0.05–1.00 mol/L) were prepared using UHP water. 10 mL of each of these solutions was contacted with the known amounts of SPFA (5–50 g/L) in a 100 ml conical flask at 298 K and 150 rpm for 2 h. Following the equilibrium, the mixture was centrifuged at 5000 rpm for 5 min to split up the phases. Then, the aqueous phase was carefully removed and analyzed for the amount of acid remained. The amount of solute adsorbed by SPFA at equilibrium (q_e) was determined by Eq. (1). In addition, the efficiency of the adsorption process can be calculated using Eq. (2).

$$q_e = \frac{C_0 - C_e}{m} \times V_s \quad (1)$$

$$\text{Adsorption Efficiency}(\%) = \frac{(C_0 - C_e)}{C_0} \times 100 \quad (2)$$

where q_e (mmol/g) is the adsorption capacity at equilibrium, C_0 and C_e (mol/L) are the initial and equilibrium concentration of the acid, respectively, m (g) represents the mass of SPFA and V_s (L) is the volume of the aqueous solution.

2.6. Thermodynamics and isotherm models

In order to detect the influence of temperature on the adsorption process, thermodynamic experiments were carried out at different initial values. The temperature of the separation process was changed between 298 and 318 K in the shaker bath. The samples were also settled at that temperature. The concentrations of the acids in the aqueous phases before and after the separation process were measured. The data were employed during the calculations of the thermodynamic parameters.

Three different isotherm models were applied to the equilibrium data in order to obtain information about the distribution of the acid molecules on the SPFA [33,34]. They are Langmuir, Freundlich, and Temkin isotherm models. The Langmuir isotherm model is the most commonly used one for the processes that occur in liquid phases. The theory assumes that the adsorption process happens at specific homogeneous sites on the adsorbent surface. Furthermore, it asserts monolayer adsorption and assumes that the

interactions between the adsorbed molecules are negligible [35,36]. The maximum capacity of the adsorbent can also be determined using the Langmuir isotherm equation. Furthermore, the favorability of the process can be clarified by using the calculation of the dimensionless separation factor according to this isotherm model. The Freundlich isotherm model is used to describe the systems having heterogeneous surfaces [37]. The third, Temkin isotherm model suggests that the heat of adsorption of all molecules on the surface linearly decreases with the coverage [38].

3. Results and discussion

3.1. Characterization

The characterizations of the raw and loaded SPFA were carried out by FTIR and SEM-EDX. The FTIR spectra give information about the functional groups and types of chemical bonds that exist or can form on the fly ash surface through the adsorption process [39]. The FTIR spectra of SPFA and acid-loaded SPFA were displayed in Fig. 1 and broadband between 3,222 and 3,500 cm^{-1} was the indication of the presence of the hydroxyl group on the SPFA surface [40]. The peaks at 2,883 and 2,351 cm^{-1} in raw SPFA shifted to 2,895; 2,342; 2,888; and 2,342 cm^{-1} in FA-loaded and AA-loaded SPFA, respectively. These peaks were due

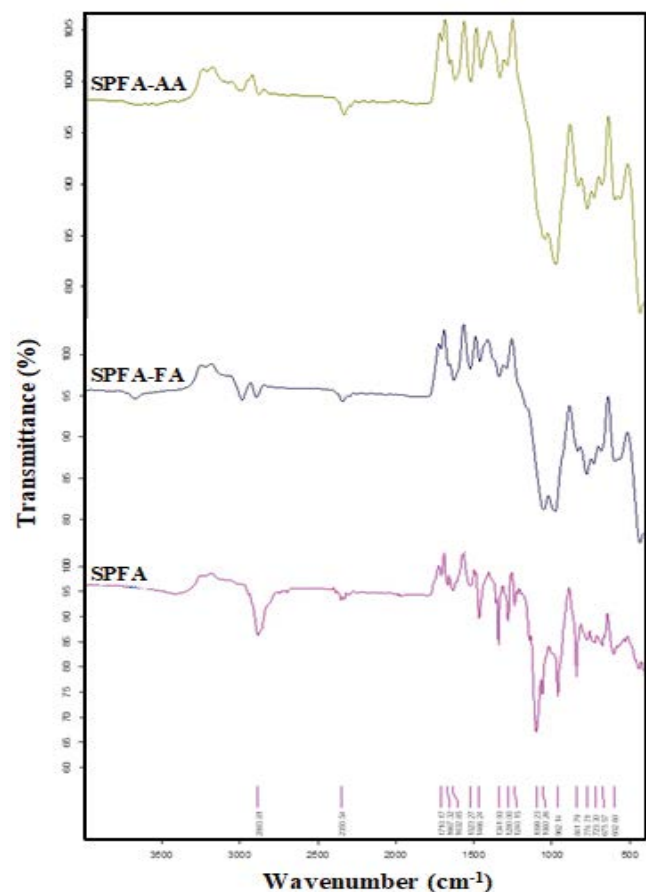


Fig. 1. FTIR spectra of the SPFA and FA loaded and AA loaded-SPFA.

to C–H stretching in aliphatic hydrocarbons and the fundamental bending of H_2O molecules corresponded to a sharp peak at $\sim 1,630\text{ cm}^{-1}$ [40]. The band at $\sim 1,340\text{ cm}^{-1}$ could be related to the rocking vibration of CH [41]. The peaks at 1,099; 842; and 458 cm^{-1} were assigned to the stretching, bending and out of the plane of Si–O bonds, respectively [42]. The shape and position of the peak that appeared at $1,099\text{ cm}^{-1}$ indicated the presence of SiO_2 with a stoichiometric structure [42]. This peak disappeared in the FA-loaded and AA-loaded SPFA indicating a change in the bonds. Consequently, the adsorption process occurred and SiO_2 can be an effective site for the adsorption of carboxylic acids.

The microstructure of SPFA before and after the adsorption process was characterized by using SEM (Fig. 2). It was observed that the SPFA particles were irregular in

shape and the adsorbent has a rough and porous surface. The differences in the surface morphology of raw and acid-loaded SPFA confirmed the presence of the acid molecules on the SPFA surface. According to the EDX analysis (Fig. 3), the main elements in the SPFA were O, Ca, Si and Al. The presence of C, N, Na, S, Fe, K and Mg were also detected (Table 1).

3.2. Effect of contact time and kinetic studies

Equilibration time has great importance for time-dependent operations. Determination of the equilibration time is useful to clarify the rate of the process, which is needed for the design of a separation event [43,44]. The results of the experimental kinetic studies on the removal

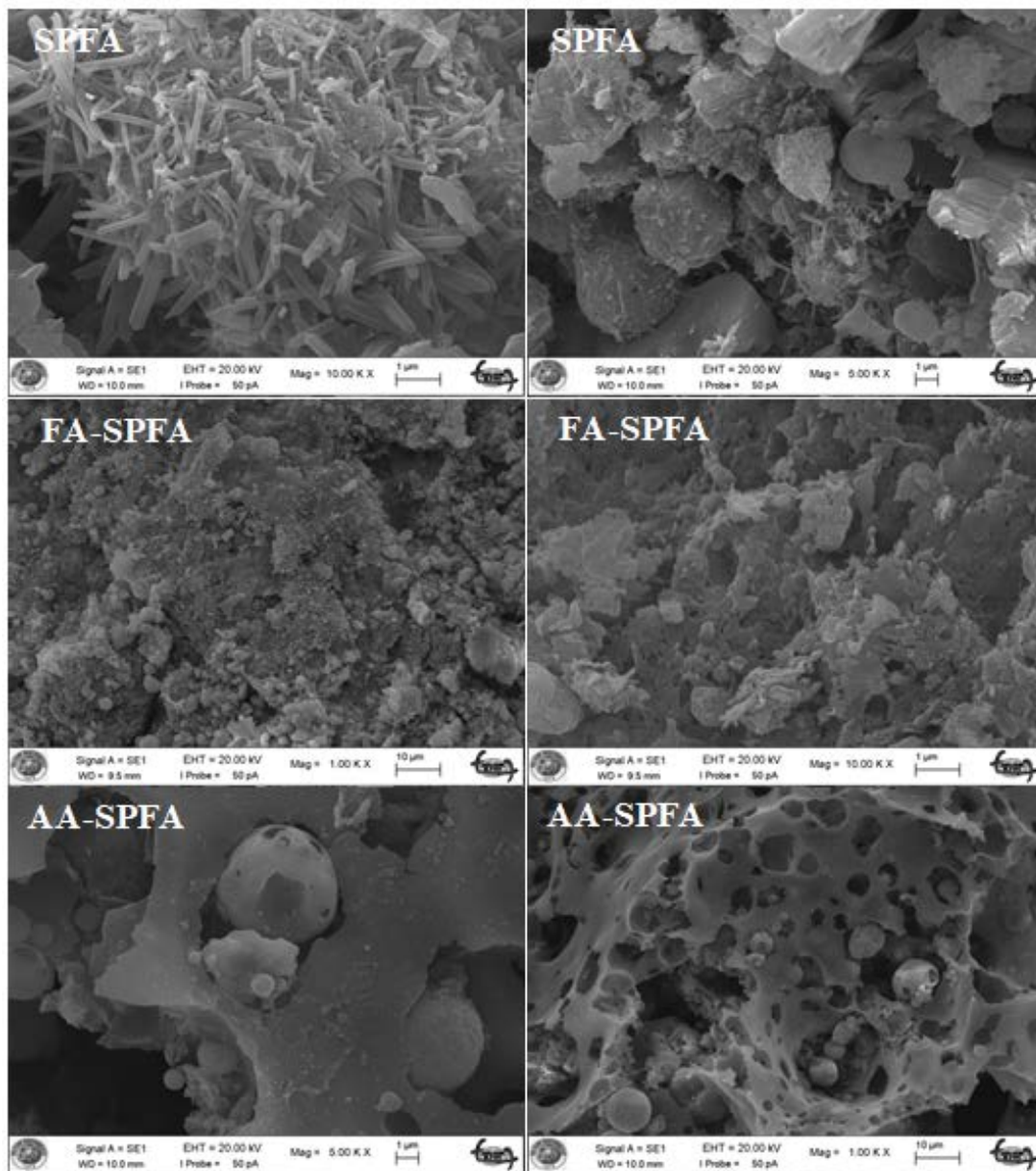


Fig. 2. SEM images of the SPFA and acid loaded-SPFA.

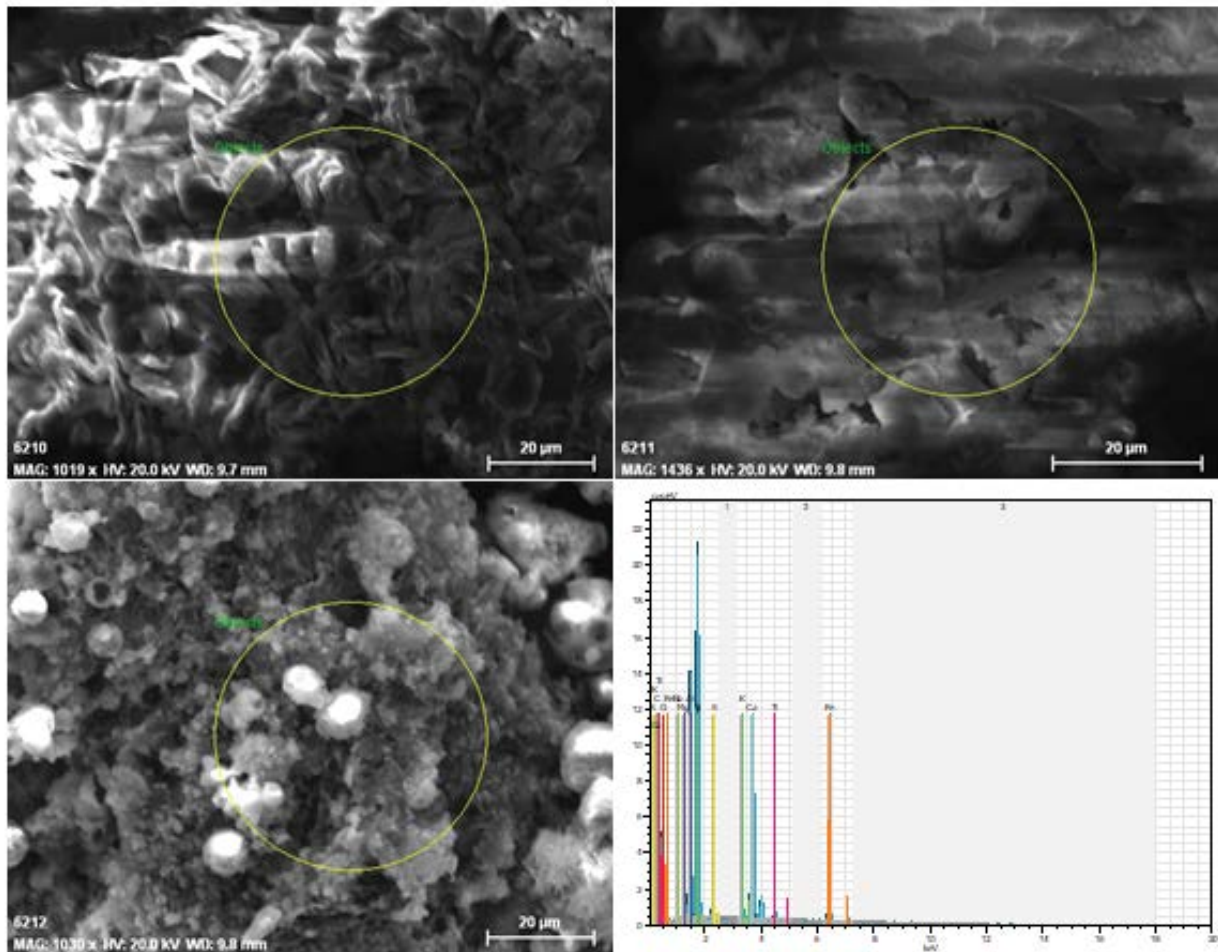


Fig. 3. SEM images and EDX micrograph of SPFA.

Table 1
The percent composition of the elements in the SPFA (results of SEM-EDX analysis)

Element	SPFA (wt.%)
O	47.30
Ca	36.67
Si	8.08
Al	3.33
C	0.45
N	1.76
Na	0.49
S	0.45
Fe	0.57
K	0.58
Mg	0.31

of AA and FA from aqueous solutions using SPFA at 298 K are illustrated in Fig. 4. The figure also helped to determine the equilibrium time. Initial concentrations of the carboxylic acids (AA or FA) were 0.25 mol/L, while adsorbent dose

was kept constant to be 20 g/L. It was observed that the adsorption rate was very fast at the initial stage of the contact period, and thereafter, it became slower while reaching the equilibrium. It is clear that a large number of unoccupied sites were available on the surface for adsorption at the beginning. Later, the free surface sites left were very hard to be occupied due to the repulsive forces between the solute molecules [45]. It can be seen from Fig. 4 that the adsorption equilibrium was achieved in 70 min for AA and 60 min for FA.

In order to analyze the kinetics of the adsorption of AA and FA onto SPFA, four kinetic models Elovich, PFO, PSO, and ID were applied to the relevant data. The expressions of these models are given below [Eqs. (3)–(6)]. The Elovich model has been satisfactorily applied to most of the chemisorption operations [Eq. (3)]. The model is generally compatible with the slow adsorption processes [46–48]. The PFO model was proposed by Lagergren [49] and this equation [Eq. (4)] is the most commonly used rate equation in liquid phase sorption processes. The PSO kinetic model suggests that the adsorption process is also controlled by chemisorption and is represented by Eq. (5) [50,51]. Weber–Morris equation [Eq. (6)] can be used to evaluate and characterize the effect of film

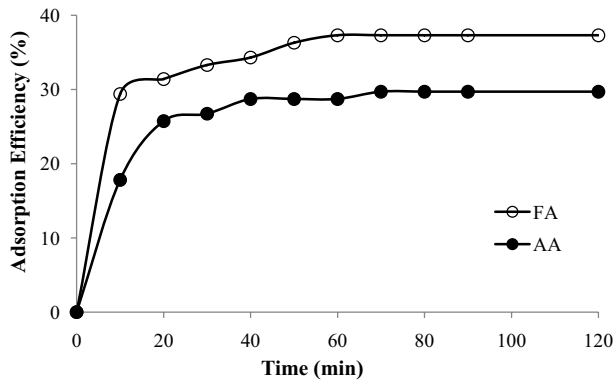


Fig. 4. Determination of the equilibration time for the adsorption of AA and FA using SPFA (initial acid concentration: 0.25 mol/L; adsorbent dose: 20 g/L; temperature: 298 K).

Table 2

Constants and R^2 values of the kinetic models for the adsorption of AA and FA by SPFA (initial acid concentration: 0.25 mol/L; adsorbent dose: 20 g/L; temperature: 298 K)

Kinetic models	Constants	Acetic acid	Formic acid
Elovich model	α	4.791	130.823
	β	0.708	0.558
	R^2	0.8776	0.9654
Pseudo-first-order (PFO) model	q_e	1.620	1.805
	k_1	0.044	0.042
	R^2	0.8501	0.9320
Pseudo-second-order (PSO) model	q_e	3.957	5.020
	k_2	0.050	0.043
	R^2	0.9987	0.9990
Intraparticle diffusion (ID) model	k_{id}	0.1577	0.1415
	I	2.3394	3.4561
	R^2	0.6635	0.8509

and intra-particle diffusion resistance on the adsorption kinetics [52].

$$\text{Elovich } \frac{dq_t}{dt} = \alpha \times \exp(-\beta \times q_t) \quad (3)$$

$$\text{PFO } \frac{dq_t}{dt} = k_1 \times (q_e - q_t) \quad (4)$$

$$\text{PSO } \frac{dq_t}{dt} = k_1 \times (q_e - q_t)^2 \quad (5)$$

$$\text{ID } q_t = k_{id} \cdot t^{1/2} + I \quad (6)$$

where q_e and q_t (mmol/g) are the adsorption capacity values at equilibrium and time t , respectively, t (min) refers to time, α (mmol/g min) represents the initial adsorption rate, β (g/mmol) is the Elovich desorption constant, k_1 (min^{-1}),

k_2 (g/mmol min), and k_{id} (mmol/g min) denote the PFO, PSO, and ID rate constants, respectively, and I (mmol/g) expresses the boundary layer diffusion effects.

The values of the model constants were calculated using the slopes and intercepts of the figures obtained by the appropriate linearization of these expressions. The R^2 values obtained for the adsorption of AA onto SPFA with Elovich, PFO, PSO and ID models were 0.8776, 0.8501, 0.9987, and 0.6635, respectively (Table 2). They were 0.9654, 0.9320, 0.9990, and 0.8509, respectively, for the adsorption of FA by SPFA. According to the results, the PSO kinetic model was more likely to be able to predict the behavior of the adsorption process for AA and FA onto SPFA. In addition, the experimental ($q_e = 3.96$ and 5.02 mmol/g) and calculated ($q_e = 4.10$ and 5.00 mmol/g) adsorption capacities for the adsorption of AA and FA by SPFA, respectively, showed good agreements. This means that the PSO model is closely related to the adsorption data. Moreover, the I value gives an idea about the thickness of the boundary layer as the larger the intercept, the greater the contribution of the surface sorption in the rate-controlling step [53,54]. The deviation of the straight line might occur due to the variation in the rate of the mass transfer during the process. This deviation can also show that pore diffusion was not the only rate-controlling step, and some other mechanisms might involve [55].

3.3. Effects of solute concentration and adsorbent dose

The isotherm curves belong to the adsorption of AA or FA onto SPFA at 30 g/L dosage level are displayed in Fig. 5. They showed that the process was fitted with Type 1 regardless of the acid type studied. This could be assigned to the Langmuir isotherm model and was a sign of a monolayer uptake.

The influence of initial acid concentration on the removal of AA or FA on the adsorption efficiency was studied in the range of 0.05–1.00 mol/L. The initial dose of the SPFA was varied between 5 and 50 g/L. Fig. 6 exhibits that adsorption efficiency reduced with the increase in initial acid concentration and the decrease in dosage level;

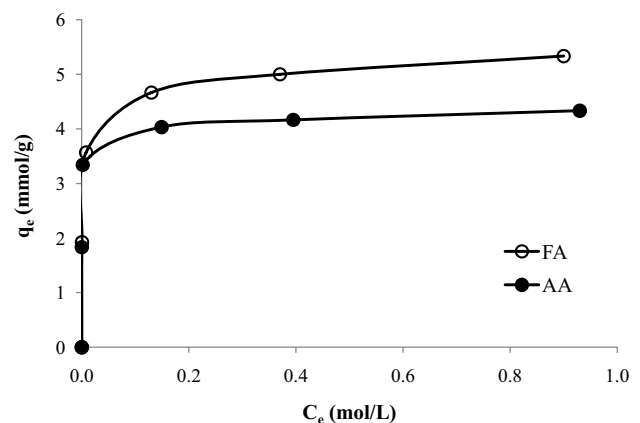


Fig. 5. Isotherm curves for the adsorption of AA and FA using SPFA (initial acid concentration: 0.05–1.00 mol/L; adsorbent dose: 30 g/L; temperature: 298 K).

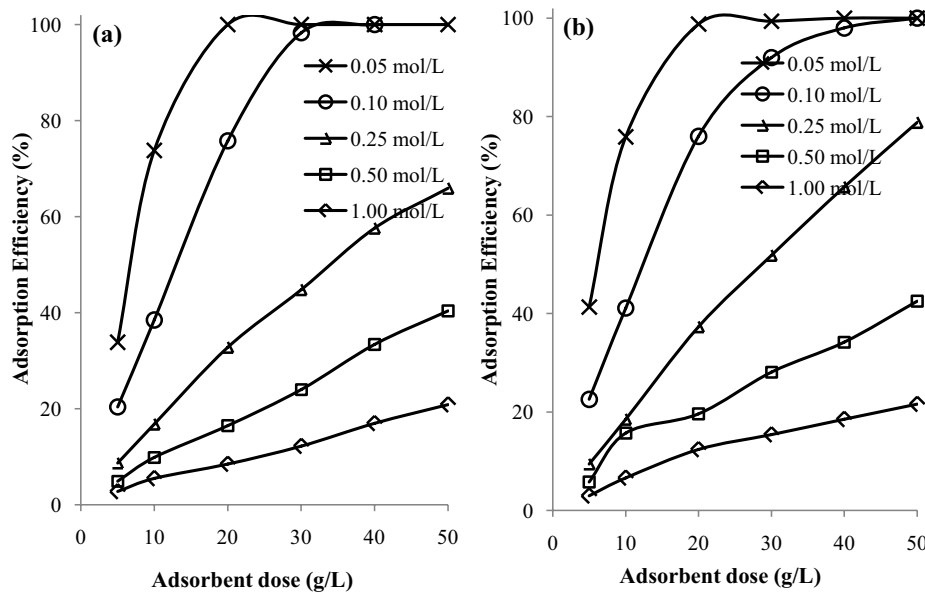


Fig. 6. Variation of adsorption efficiency with the SPFA dose for several initial acid concentrations (a) acetic acid and (b) formic acid (initial acid concentration: 0.05–1.00 mol/L; adsorbent dose: 5–50 g/L; temperature: 298 K).

however, the adsorption capacity (q_e) presented an opposite trend. This means that the adsorption process with SPFA was very effective especially with dilute solutions. Since the ratio of the solute molecules to the available sites on the sorbent surface increases at the higher concentrations, adsorption efficiency decreased with the increase in (initial) acid concentration. Higher adsorbent dosage provides a higher surface area, in other words, more available sites for the separation process [56]. The decrease in the adsorption efficiency can also be explained with the saturation of the SPFA surface.

The removal efficiencies and adsorption capacities were compared for AA and FA. The highest adsorption percentages (99.5%–100%) were obtained at the 0.05 mol/L acid concentration levels, especially at high dosage levels (Fig. 6). The trend was valid for both solutes. However, at higher initial acid concentrations, the values obtained with FA were higher than those with AA for all SPFA doses. The superiority was most apparent when the initial acid concentration was 0.25 mol/L. The highest adsorption capacity values reached in this study in the range of the parameters were 7.00 and 5.60 mmol/g for FA and AA, respectively. These q_e values were obtained when the initial dosage and acid concentrations were 5 g/L and 0.05 mol/L, respectively. These capacity values for AA and FA were in the range and mostly higher than the values previously published in the literature using several types of synthetic resins, metal oxides and fly ashes (Table 3) [12,14,20,30,57,58,62]. These results evidently showed that SPFA can be effectively used to separate these carboxylic acids from aqueous-based solutions.

3.4. Adsorption isotherms

The isotherm models are important for understanding the behavior of the adsorption process. They can indicate

the distribution of the solute molecules between the solid (adsorbed) and the liquid (non-adsorbed) phases [33,34,64]. Three different isotherm models such as Langmuir, Freundlich, and Temkin were used to investigate the characteristics of the adsorption process. The equations of these isotherm models [Eqs. (7)–(10)] are given below:

$$\text{Langmuir } q_e = Q_{\max} \cdot \frac{K_L \cdot C_e}{1 + K_L \cdot C_e} \quad (7)$$

$$R_L = \frac{1}{(1 + (K_L \cdot C_0))} \quad (8)$$

$$\text{Freundlich } q_e = K_F \cdot [C_e]^{1/n} \quad (9)$$

$$\text{Temkin } q_e = \frac{R \cdot T}{B} \cdot \ln(K_T \cdot C_e) \quad (10)$$

where q_e (mmol/g) is the adsorption capacity at equilibrium, Q_{\max} (mmol/g) refers the maximum adsorption capacity at that dosage level, K_L (L/mol) denotes the Langmuir equilibrium constant, C_e (mol/L) is the equilibrium concentration of the acid in the aqueous solution and R_L signifies the dimensionless separation factor. The process is estimated to be irreversible ($R_L = 0$), favorable ($0 < R_L < 1$), linear ($R_L = 1$) or unfavorable ($R_L > 1$) depending on the value of the separation factor [34,65]. K_F (L/mol) and n are the Freundlich adsorption capacity and intensity, respectively. Likewise explained in Langmuir, depending on the value of $1/n$, process is said to be irreversible ($1/n = 0$), favorable ($0 < 1/n < 1$) or unfavorable ($1/n > 1$). In addition, B (J/mol) and K_T (L/mol) are Temkin equilibrium-binding constant and the Temkin constant related to the adsorption heat, respectively.

Table 3
Maximum adsorption capacity (Q_{\max}) values and adsorbent/resin types for separation of FA and AA in the literature

Carboxylic acid	Adsorbent	Q_{\max} (mmol/g)	Reference
Formic acid	SPFA	7.00	Present study
Acetic acid	SPFA	5.60	Present study
Formic acid	Lewatit MP-64 (Sigma-Aldrich Co., USA)	9.63	[12]
Formic acid	Amberlite IRA-96 (Sigma-Aldrich Co., USA)	5.00	[12]
Formic acid	D-II07 (Guangzhou, China)	2.24	[14]
Formic acid	Amberlite IRA-67 (Merck Co., USA)	5.20	[20]
Acetic acid	Fly ash	5.50	[30]
Acetic acid	Indion 850 (Ion Exchange Ltd., Mumbai, India)	11.00	[57]
Acetic acid	Tulsion A-8XMP (Thermax Ltd., Pune, India)	7.00	[57]
Acetic acid	Indion 810 (Ion Exchange Ltd., Mumbai, India)	5.00	[57]
Acetic acid	330 resin (Tianjin Chemical Co., China)	1.20	[58]
Acetic acid	UiO-66	2.74	[62]

The linearization of these isotherm expressions gave the linear relationships of these isotherm models (Figs. 7 and 8). The slopes and intercepts of these figures provided the R^2 values and model constants. According to Table 4, the highest R^2 values (>0.99) were obtained with the Langmuir isotherm model for both AA and FA. This means that the model described the equilibrium data very well for the two acids studied. The calculated Q_{\max} values obtained with the Langmuir isotherm were 4.52 and 6.52 mmol/g for AA and FA, respectively. They were very close to the values experimentally obtained, which were 4.25 and 6.50 mmol/g for these two acids, respectively. It can also be added that the process was favorable for both solutes according to the R_L values.

3.5. Thermodynamic studies

The effect of temperature on the adsorption of AA and FA using SPFA is shown in Fig. 9. The influence was investigated at the adsorbent dosage of 20 g/L and in the

range of 298–318 K. It was observed that the adsorption efficiency decreased with the increase in temperature for both acids (Fig. 9). However, the influence was not significant ($p > 0.10$). Especially the values obtained at 298 and 308 K were almost the same. Those at 318 K were slightly lower than the others. The trend might be partially due to the weakening of the attractive forces between the carboxylic acids and SPFA surface with temperature [25]. The effect of temperature on the adsorption of AA or FA onto SPFA suggested that the process was exothermic. The extent of the effect did not differ for the two acids studied. The Gibbs free energy change (ΔG°), enthalpy change (ΔH°) and entropy change (ΔS°) were determined using the data and Eqs. (11)–(13).

$$\Delta G^\circ = \Delta H^\circ - T\Delta S^\circ \quad (11)$$

$$\Delta G^\circ = -R \cdot T \cdot \ln K_L \quad (12)$$

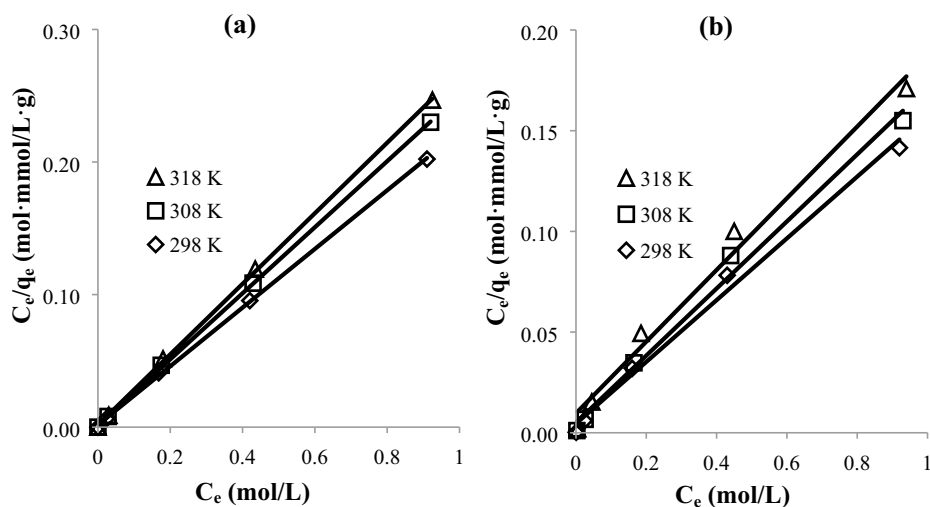


Fig. 7. Langmuir isotherm for the adsorption of AA and FA by SPFA at different temperatures (a) acetic acid and (b) formic acid (initial acid concentration: 0.05–1.00 mol/L; adsorbent dose: 20 g/L; temperature: 298–318 K).

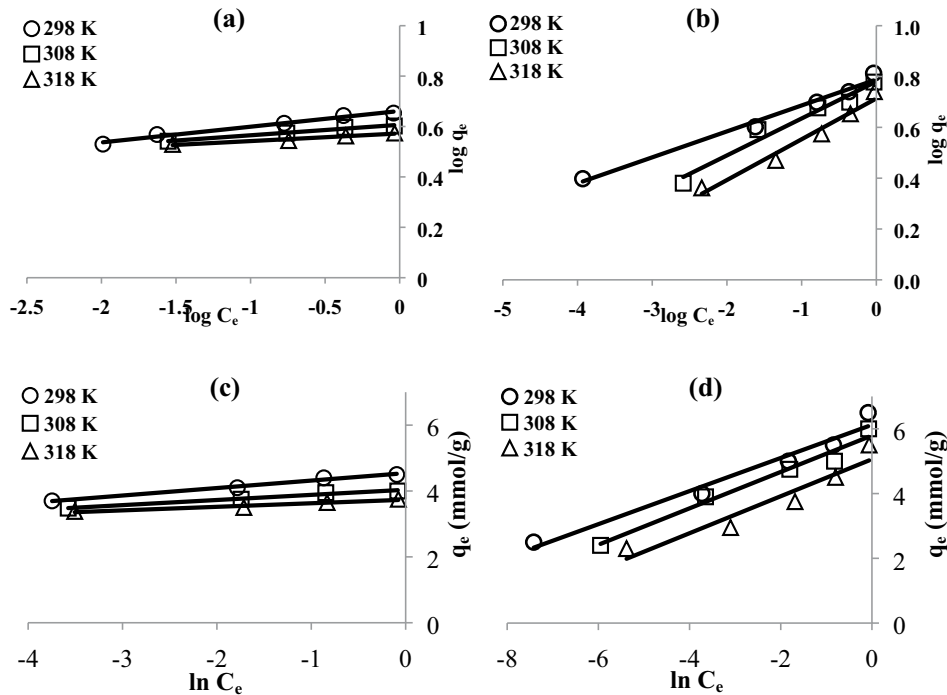


Fig. 8. Freundlich and Temkin isotherms for the adsorption of AA and FA using SPFA (a) Freundlich-AA, (b) Freundlich-FA, (c) Temkin-AA, and (d) Temkin-FA (initial acid concentration: 0.05–1.00 mol/L; adsorbent dose: 20 g/L; temperature: 298–318 K).

Table 4
 Constants and R^2 values of the isotherm models for the adsorption of AA and FA onto SPFA (initial acid concentration: 0.05–1.00 mol/L; adsorbent dose: 20 g/L; temperature: 298 K)

Isotherm model	Constants	Acetic acid	Formic acid
Langmuir	Q_{max}	4.52	6.52
	K_L	130.112	34.067
	R^2	0.9997	0.9922
Freundlich	R_L	0.008–0.131	0.027–0.367
	n	17.986	7.949
	K_F	4.556	6.344
Temkin	R^2	0.9829	0.9851
	B	0.2267	0.5113
	K_T	5.0×10^5	1.6×10^5
	R^2	0.9874	0.9653

$$\ln K_L = -\frac{\Delta H^\circ}{R \cdot T} + \frac{\Delta S^\circ}{R} \quad (13)$$

where T (K) is the temperature, K_L (L/mol) is the Langmuir equilibrium constant and R (J/mol K) is the gas constant. Table 5 shows the values of the thermodynamic parameters and K_L . According to the literature, the ΔG° value is between -20 and 0 kJ/mol if it is a physisorption process. The value is in the range of -80 to -400 kJ/mol if it is a chemisorption process [66]. The ΔG° values were between -12.062 and -12.797 kJ/mol for AA and -4.740 and -8.742 kJ/mol for FA. This means that the adsorption of AA or FA onto SPFA was

a physical event and the possible mechanism is described in Fig. 10. Their negative values indicated to the spontaneity of the process. The values of ΔH° and ΔS° were calculated by the Van't Hoff equation [Eq. (14)]. The ΔH° values were calculated to be -1.055 and -65.589 kJ/mol for AA and FA, respectively. These negative values confirmed the feasibility and exothermic nature of the adsorption process. In addition, the positive values of ΔS° showed that the randomness at the solid–liquid interface increased during the separation process.

4. Conclusions

Herein, a comparative study was presented for the separation of AA and FA from aqueous solutions by using SPFA as the adsorbent. Equilibration times were found to be about 70 and 60 min for AA and FA, respectively. For both systems, the kinetic data were observed to follow the PSO kinetic model ($R^2 > 0.998$). The calculated q_e values (4.10 and 5.00 mmol/g) were close to the experimental data (3.96 and 5.02 mmol/g) for the adsorption of AA and FA by SPFA, respectively. According to the isotherm curves, the adsorption of AA and FA onto SPFA was fitted with Type 1. The adsorption efficiency increased with the increase in SPFA dosage and decreased with the acid concentration. The adsorption capacities and removal efficiencies obtained with FA ($Q_{max} = 7.00$ mmol/g) were higher than the ones with AA ($Q_{max} = 5.6$ mmol/g). These values were in the range and mostly higher than the ones formerly reported in the literature using several types of synthetic resins, metal oxides and fly ashes. Equilibrium data were in consistency with the Langmuir isotherm model for both AA

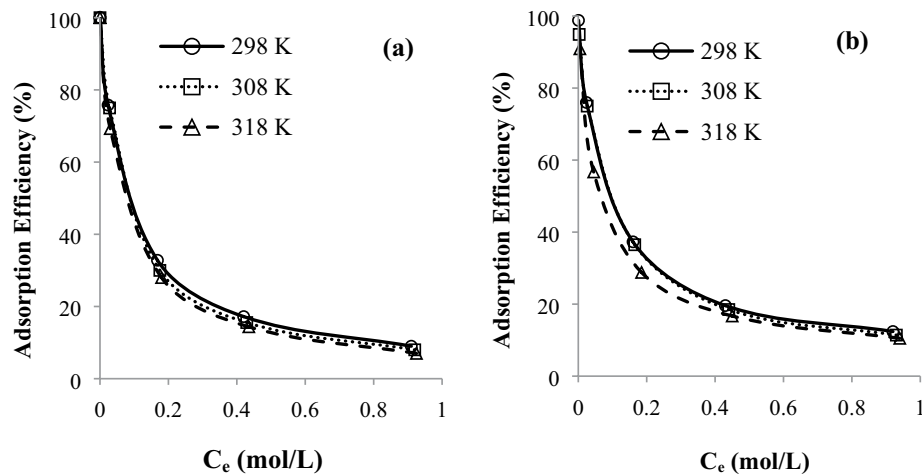


Fig. 9. Effect of temperature on the adsorption of AA and FA using SPFA (a) acetic acid and (b) formic acid (initial acid concentration: 0.05–1.00 mol/L; adsorbent dose: 20 g/L).

Table 5

Thermodynamic parameters for the adsorption of AA and FA using SPFA (initial acid concentration: 0.05–1.00 mol/L; adsorbent dose: 20 g/L; temperature: 298–318 K)

Acid type	T (K)	$\ln K_L$	ΔG° (kJ/mol)	ΔH° (kJ/mol)	ΔS° (J/mol K)
Acetic acid	298	4.8684	-12.062	-1.055	36.958
	308	4.8646	-12.457		
	318	4.8405	-12.797		
Formic acid	298	3.5283	-8.742	-65.589	-188.703
	308	3.5056	-8.977		
	318	1.7928	-4.740		

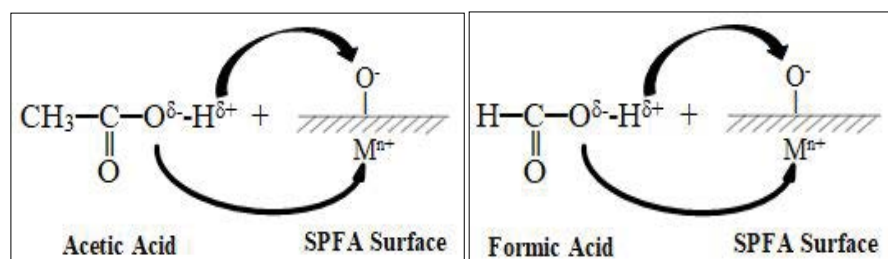


Fig. 10. Proposed mechanism for the adsorption of acetic acid and formic acid onto the SPFA surface (inspired by Iraola-Arregui et al. [67]).

and FA ($R^2 > 0.99$). Moreover, the values of the separation factor were between 0 and 1 indicating that the process was favorable.

Thermodynamics showed that the efficiency was slightly but negatively influenced by the temperature. For both AA and FA adsorptions, the changes in the enthalpy and Gibbs free energy were at the range of physisorption and had negative values, which meant that the process was exothermic and spontaneous regardless of the acid type studied. The entropy values signified that the randomness at the interface increased during the separation process. This comparative study showed that the SPFA can be efficiently used as an adsorbent for the separation of AA and FA from aqueous solutions.

Funding

The authors acknowledge Selçuk University for the funding through the Scientific Research Projects Coordination Unit under the Grant Number, 16201046.

References

- [1] İ. İnci, Ş.S. Bayazit, Y.S. Aşçı, Solid-liquid equilibrium of glycolic acid with alumina, *Desal. Water Treat.*, 56 (2015) 3122–3127.
- [2] Ö. Özcan, İ. İnci, Y.S. Aşçı, Ş.S. Bayazit, Oxalic acid removal from wastewater using multi-walled carbon nanotubes: kinetic and equilibrium analysis, *J. Dispersion Sci. Technol.*, 38 (2017) 65–69.

- [3] M.E. Marti, Recovery of formic acid by reactive extraction using an environmentally-friendly solvent, *Selçuk Univ. J. Eng. Sci. Technol.*, 5 (2017) 26–37.
- [4] S.O. Adio, M.H. Omar, M. Asif, T.A. Saleh, Arsenic and selenium removal from water using biosynthesized nanoscale zero-valent iron: a factorial design analysis, *Process Saf. Environ.*, 107 (2017) 518–527.
- [5] A.A. Basaleh, M.H. Al-Malack, T.A. Saleh, Methylene blue removal using polyamide-vermiculite nanocomposites: kinetics, equilibrium and thermodynamic study, *J. Environ. Chem. Eng.*, 7 (2019) 103107.
- [6] T.A. Saleh, I. Ali, Synthesis of polyamide grafted carbon microspheres for removal of rhodamine B dye and heavy metals, *J. Environ. Chem. Eng.*, 6 (2018) 5361–5368.
- [7] H. Cheung, R.S. Tanke, G.P. Torrence, *Acetic Acid*, Ullmann's Encyclopedia of Industrial Chemistry, Berlin, 2011.
- [8] H. Zeidan, Selective Recovery of Levulinic, Acetic and Formic Acids from Multi Acid Aqueous Solutions by Reactive Extraction, Ph.D. Thesis, Selçuk University, Konya, Turkey, 2019.
- [9] M.E. Marti, Solvent modification effect on the physical and chemical extraction of acetic acid, *Sep. Sci. Technol.*, 51 (2016) 1806–1816.
- [10] W. Reutemann, H. Kieczka, *Formic Acid*, Ullmann's Encyclopedia of Industrial Chemistry, Berlin, 2011.
- [11] T. Brouwer, M. Blahusiak, K. Babic, B. Schuur, Reactive extraction and recovery of levulinic acid, formic acid and furfural from aqueous solutions containing sulphuric acid, *Sep. Purif. Technol.*, 185 (2017) 186–195.
- [12] H. Zeidan, M.E. Marti, Separation of formic acid from aqueous solutions onto anion exchange resins: equilibrium, kinetic, and thermodynamic data, *J. Chem. Eng. Data*, 64 (2019) 2718–2727.
- [13] C.B. Rasrendra, B. Girisuta, H.H. van de Bovenkamp, J.G.M. Winkelman, E.J. Leijenhorst, R.H. Venderbosch, M. Windt, D. Meier, H.J. Heeres, Recovery of acetic acid from an aqueous pyrolysis oil phase by reactive extraction using tri-*n*-octylamine, *Chem. Eng. J.*, 176–177 (2011) 244–252.
- [14] X.Q. Lin, L. Xiong, C. Huang, X.Y. Yang, H.J. Guo, X.F. Chen, X.D. Chen, Sorption behavior and mechanism investigation of formic acid removal by sorption using an anion-exchange resin, *Desal. Water Treat.*, 57 (2016) 366–381.
- [15] D. Painer, S. Lux, M. Siebenhofer, Recovery of formic acid and acetic acid from waste water using reactive distillation, *Sep. Sci. Technol.*, 50 (2015) 2930–2936.
- [16] C. López-Garzón, A.J.J. Straathof, Recovery of carboxylic acids produced by fermentation, *Biotechnol. Adv.*, 32 (2014) 873–904.
- [17] S.-T. Yang, H.J. Huang, A. Tay, W. Qin, L. De Guzman, E.C. San Nicolas, Chapter 16 – Extractive Fermentation for the Production of Carboxylic Acids, S.-T. Yang, Ed., *Bioprocessing for Value-Added Products from Renewable Resources: New Technologies and Applications*, Elsevier, Dublin, OH, 2007, pp. 421–446.
- [18] D. Datta, S. Kumar, H. Uslu, Status of the reactive extraction as a method of separation, *J. Chem.*, (2015) 1–16, <https://doi.org/10.1155/2015/853789>.
- [19] A.A. Garcia, C.J. King, The use of basic polymer sorbents for the recovery of acetic acid from dilute aqueous solution, *Ind. Eng. Chem. Res.*, 28 (1989) 204–212.
- [20] H. Uslu, Adsorption equilibria of formic acid by weakly basic adsorbent Amberlite IRA-67: equilibrium, kinetics, thermodynamic, *Chem. Eng. J.*, 155 (2009) 320–325.
- [21] H.A. Asmaly, Ihsanullah, B. Abussaud, T.A. Saleh, T. Laoui, V.K. Gupta, M.A. Atieh, Adsorption of phenol on aluminum oxide impregnated fly ash, *Desal. Water Treat.*, 57 (2016) 6801–6808.
- [22] R. Rajamma, R.J. Ball, L.A.C. Tarelho, G.C. Allen, J.A. Labrincha, V.M. Ferreira, Characterization and use of biomass fly ash in cement-based materials, *J. Hazard. Mater.*, 172 (2009) 1049–1060.
- [23] Y. Wen, Z.R. Tang, Y. Chen, Y.X. Gu, Adsorption of Cr(VI) from aqueous solutions using chitosan-coated fly ash composite as biosorbent, *Chem. Eng. J.*, 175 (2012) 110–116.
- [24] O.S. Fatoki, O.S. Ayanda, F.A. Adekola, B.J. Ximba, Sorption of triphenyltin chloride to $n\text{Fe}_3\text{O}_4$ fly ash, and $n\text{Fe}_3\text{O}_4$ /fly ash composite material in seawater, *Clean – Soil Air Water*, 42 (2014) 472–479.
- [25] K.K. Panday, G. Prasad, V.N. Singh, Copper(II) removal from aqueous solutions by fly ash, *Water Res.*, 19 (1985) 869–873.
- [26] A. Akgerman, M. Zardkoobi, Adsorption of phenolic compounds on fly ash, *J. Chem. Eng. Data*, 41 (1996) 185–187.
- [27] N. Öztürk, D. Kavak, Adsorption of boron from aqueous solutions using fly ash: batch and column studies, *J. Hazard. Mater.*, 127 (2005) 81–88.
- [28] I.J. Alinnor, Adsorption of heavy metal ions from aqueous solution by fly ash, *Fuel*, 86 (2007) 853–857.
- [29] N. Kannan, A. Xavier, New composite mixed adsorbents for the removal of acetic acid by adsorption from aqueous solutions – a comparative study, *Toxicol. Environ. Chem.*, 79 (2001) 95–107.
- [30] S.C. Nawle, S.V. Patil, Experimental studies on acetic acid removal from waste water using fly ash, *Nirma Univ. Int. Conf. Curr. Trends Technol. Proc. Chem.*, 26 (2011) 1–4.
- [31] A.B. Soni, A. Keshav, V. Verma, S. Suresh, Removal of glycolic acid from aqueous solution using bagasse flyash, *Int. J. Environ. Res.*, 6 (2012) 297–308.
- [32] R. Scherer, A.C.P. Rybka, C.A. Ballus, A.D. Meinhart, J.T. Filho, H.T. Godoy, Validation of a HPLC method for simultaneous determination of main organic acids in fruits and juices, *Food Chem.*, 135 (2012) 150–154.
- [33] I.A.W. Tan, A.L. Ahmad, B.H. Hameed, Adsorption of basic dye on high-surface-area activated carbon prepared from coconut husk: equilibrium, kinetic and thermodynamic studies, *J. Hazard. Mater.*, 154 (2008) 337–346.
- [34] M. Pirsahab, Z. Rezai, A.M. Mansouri, A. Rastegar, A. Alahabadi, A.R. Sani, K. Sharafi, Preparation of the activated carbon from India shrub wood and their application for methylene blue removal: modeling and optimization, *Desal. Water Treat.*, 57 (2015) 5888–5902.
- [35] I. Langmuir, The constitution and fundamental properties of solids and liquids. Part I. Solids, *J. Am. Chem. Soc.*, 38 (1916) 2221–2295.
- [36] R.P. Han, P. Han, Z.H. Cai, Z.H. Zhao, M.S. Tang, Kinetics and isotherms of neutral red adsorption on peanut husk, *J. Environ. Sci.*, 20 (2008) 1035–1041.
- [37] H.M.F. Freundlich, Über die adsorption in losungen (Adsorption in solution), *Z. Phys. Chem.*, 57 (1906) 385–490.
- [38] M. Temkin, V. Pyzhev, Kinetics of ammonia synthesis on promoted iron catalysts, *Acta Phys.*, 12 (1940) 217–222.
- [39] B. Acemioglu, Adsorption of Congo red from aqueous solution onto calcium-rich fly ash, *J. Colloid Interface Sci.*, 274 (2004) 371–379.
- [40] Saakshy, K. Singh, A.B. Gupta, A.K. Sharma, Fly ash as low cost adsorbent for treatment of effluent of handmade paper industry-kinetic and modelling studies for direct black dye, *J. Cleaner Prod.*, 112 (2016) 1227–1240.
- [41] R.N. Oliveira, M.C. Mancini, F.C.S. de Oliveira, T.M. Passos, B. Quilty, R.M. da Silva Moreira Thiré, G.B. McGuinness, FTIR analysis and quantification of phenols and flavonoids of five commercially available plants extracts used in wound healing, *Rev. Mater.*, 21 (2016) 767–779.
- [42] B. Shokri, M.A. Firouzjah, S.I. Hosseini, FTIR Analysis of Silicon Dioxide Thin Film Deposited by Metal Organic-Based PECVD, Proceedings of 19th International Symposium on Plasma Chemistry Society, Bochum, Germany, 2009.
- [43] S.H. Chen, J. Zhang, C.L. Zhang, Q.Y. Yue, Y. Li, C. Li, Equilibrium and kinetic studies of methyl orange and methyl violet adsorption on activated carbon derived from *Phragmites australis*, *Desalination*, 252 (2010) 149–156.
- [44] T.A. Saleh, M. Tuzen, A. Sari, Polyamide magnetic palygorskite for the simultaneous removal of Hg(II) and methyl mercury; with factorial design analysis, *J. Environ. Manage.*, 211 (2018) 323–333.
- [45] D.P. Xu, C.J. Gu, X. Chen, Adsorption and removal of Acid Red 3R from aqueous solution using flocculent humic acid isolated from lignite, *Procedia Environ. Sci.*, 18 (2013) 127–134.
- [46] M.J.D. Low, Kinetics of chemisorption of gases on solids, *Chem. Rev.*, 60 (1960) 267–312.

- [47] S.Y. Elovich, O.G. Larinov, Theory of adsorption from solutions of non-electrolytes on solid (I) equation adsorption from solutions and the analysis of its simplest form, (II) verification of the equation of adsorption isotherm from solutions, *Izvestiya Akademii Nauk. SSSR, Otdelenie Khimicheskikh Nauk*, 2 (1962) 209–216.
- [48] Q. Li, J.M. Xing, W.L. Li, Q.F. Liu, Z.G. Su, Separation of succinic acid from fermentation broth using weak alkaline anion exchange adsorbents, *Ind. Eng. Chem. Res.*, 48 (2009) 3595–3599.
- [49] S.Y. Lagergren, Zur theorie Der Sogenannten adsorption geloster stoffe, *Kungliga Svenska Vetenskapsakademiens*, 24 (1898) 1–39.
- [50] Y.S. Ho, G. McKay, Pseudo-second-order model for sorption processes, *Process Biochem.*, 34 (1999) 451–465.
- [51] C.W. Cheung, J.F. Porter, G. McKay, Elovich equation and modified second-order equation for sorption of cadmium ions onto bone char, *J. Chem. Technol. Biotechnol.*, 75 (2000) 963–970.
- [52] H. Qiu, L. Lv, B.-c. Pan, Q.-j. Zhang, W.-m. Zhang, Q.-x. Zhang, Critical review in adsorption kinetic models, *J. Zhejiang Univ. – Sci. A*, 10 (2009) 716–724.
- [53] D. Kavitha, C. Namasivayam, Experimental and kinetic studies on methylene blue adsorption by coir pith carbon, *Bioresour. Technol.*, 98 (2007) 14–21.
- [54] E. Demirbaş, M.Z. Nas, Batch kinetic and equilibrium studies of adsorption of Reactive Blue 21 by fly ash and sepiolite, *Desalination*, 243 (2009) 8–21.
- [55] A. Khaled, A. El Nemr, A. El-Sikaily, O. Abdelwahab, Treatment of artificial textile dye effluent containing Direct Yellow 12 by orange peel carbon, *Desalination*, 238 (2009) 210–232.
- [56] I.D. Mall, V.C. Srivastava, N.K. Agarwal, Removal of Orange-G and Methyl Violet dyes by adsorption onto bagasse fly ash—kinetic study and equilibrium isotherm analyses, *Dyes Pigm.*, 69 (2006) 210–223.
- [57] H.M. Anasthas, V.G. Gaikar, Adsorption of acetic acid on ion-exchange resins in non-aqueous conditions. *React. Funct. Polym.*, 47 (2001) 23–35.
- [58] H.S. Lv, Y.P. Sun, M.H. Zhang, Z.F. Geng, M.M. Ren, Removal of acetic acid from fuel ethanol using ion-exchange resin, *Energy Fuels*, 26 (2012) 7299–7307.
- [59] B.-J. Liu, Z.-J. Hu, Q.-L. Ren, Single-component and competitive adsorption of levulinic/formic acids on basic polymeric adsorbents, *Colloids Surf., A*, 339 (2009) 185–191.
- [60] O. Gamba, H. Noei, J. Pavelec, R. Bliem, M. Schmid, U. Diebold, A. Stierle, G.S. Parkinson, Adsorption of formic acid on the $\text{Fe}_3\text{O}_4(001)$ surface, *J. Phys. Chem. C*, 119 (2015) 20459–20465.
- [61] F.C. Calaza, T.-L. Chen, D.R. Mullins, Y. Xu, S.H. Overbury, Reactivity and reaction intermediates for acetic acid adsorbed on $\text{CeO}_2(111)$, *Catal. Today*, 253 (2015) 65–76.
- [62] H.H. Zhang, X.Y. Lan, P. Bai, X.H. Guo, Adsorptive removal of acetic acid from water with metal-organic frameworks, *Chem. Eng. Res. Des.*, 111 (2016) 127–137.
- [63] T.A. Saleh, Naeemullah, M. Tuzen, A. Sari, Polyethylenimine modified activated carbon as novel magnetic adsorbent for the removal of uranium from aqueous solution, *Chem. Eng. Res. Des.*, 117 (2017) 218–227.
- [64] W. Zhao, S.J. Carey, S.E. Morgan, C.T. Campbell, Energetics of adsorbed formate and formic acid on Ni(111) by calorimetry, *J. Catal.*, 352 (2017) 300–304.
- [65] G. Annadurai, L.Y. Ling, J.-F. Lee, Adsorption of reactive dye from an aqueous solution by chitosan: isotherm, kinetic and thermodynamic analysis, *J. Hazard. Mater.*, 152 (2008) 337–346.
- [66] Z. Bekçi, Y. Seki, L. Cavas, Removal of malachite green by using an invasive marine alga *Caulerpa racemosa* var. *cylindracea*, *J. Hazard. Mater.*, 161 (2009) 1454–1460.
- [67] I. Iraola-Arregui, H. Potgieter, C.M. Liauw, Evaluation of coupling agents in poly(propylene)/fly ash composites: effect on processing and mechanical properties, *Macromol. Mater. Eng.*, 296 (2011) 810–819.